NUMERICAL SIMULATION OF THE RTM LIGHT MANUFACTURING PROCESS

J. Timms[1], S. Bickerton[1]*, P.A. Kelly[2]
[1] Department of Mechanical Engineering, The University of Auckland, Auckland, New Zealand,
[2] Department of Engineering Science, The University of Auckland, Auckland, New Zealand
* Corresponding author (s.bickerton@auckland.ac.nz)

Keywords: RTM Light, Infusion, VARTM, Simulation, Experimental

1 Introduction

Liquid Composite Moulding (LCM) describes a range of composites manufacturing processes where dry fibrous reinforcements are compacted in a mould before being impregnated with a liquid thermosetting matrix. Although all LCM processes use closed moulds, they can vary in stiffness from fully rigid to fully flexible, with the heavy tooling of Resin Transfer Moulding (RTM) and Compression Resin Transfer Moulding (CRTM) processes at one end of the spectrum, and the thin flexible films used in Resin Infusion (a.k.a. VARTM) at the other.

The RTM Light manufacturing process differs from RTM by replacing one rigid mould half with a lighter, less rigid component (Fig. 1). The flexible mould is often manufactured from an isotropic glass fibre composite, and clamping is usually provided by application of vacuum to a region at the periphery of the mould cavity. Resin flow is driven by a cavity vacuum, an external injection system, or a combination of the two. RTM Light can allow for significant reductions in tooling costs as compared to RTM. This is at the expense of introducing some compliance into the mould, but still allows for higher injection pressures and final part quality than flexible film processes.

This paper focuses on the development of a 2D numerical simulation of the RTM Light process, capable of predicting resin flow front and laminate thickness evolution during filling.

2 Simulation approach

Numerical simulations of rigid tool LCM processes have been in development for over 20 years, with several academic and commercial packages now available [1, 2]. In the last decade a number of flexible tool simulations have also been developed [3, 4], along with numerous advances in the areas of computational efficiency, process optimization, and part quality prediction [4, 5].

These simulations are predominantly based on the Finite Element/Control Volume (FE/CV) method, because of its efficiency and the ease with which it can model complex part geometries [1, 4, 6]. This allows for fast filling simulations of industrially relevant parts.

The RTM Light simulation presented in this paper uses a coupled Finite Element scheme. A mesh of elements modelling Darcian flow through deformable porous media (the 'flow domain') is coupled with a second mesh of structural elements that represents the deformable mould (the 'structural' domain).

3 Fluid flow problem

RTM Light involves the flow of resin through a (typically) thin fibrous preform in a deformable mould. This type of flow may be modelled as Darcian flow through thickness-varying porous media, which is governed by the partial differential equation

$$\nabla \cdot \left(\frac{\mathbf{K}}{\mu} \nabla p \right) = \frac{\dot{h}}{h} \qquad (1)$$

where K is the permeability tensor, μ is the fluid viscosity, p is the fluid pressure, h is the preform height and $\dot{h}$ its first time derivative.

A conventional quasi-static FE/CV approach is adopted for the mould filling process, whereby p is solved over the saturated domain using the Galerkin finite element method. The fluid flux is then calculated at the free boundary, and the flow front is advanced by choosing a time step that results in the complete saturation of at least one CV.

Non-conforming linear triangle elements are used so that the control volumes can be formed by the elements themselves. It was shown in [2] for the rigid mould case that non-conforming triangles

conserve fluid mass both within and between elements. However, this does not hold in general for thickness varying elements, so a modification to the fluid flux $\mathbf{q}_a$ proposed by Kelly [7] has been adopted:

$$\mathbf{q}_a(\mathbf{x}) = -\frac{\mathbf{K}}{\mu}\nabla p_{FE} + \frac{-\dot{h}/h}{2}(\mathbf{x} - \mathbf{x}_B) \qquad (2)$$

where $\mathbf{x}_B$ is the barycentre of the element. Equation 2 ensures intra-element mass conservation and, in the case of constant or linearly varying forcing terms, flux continuity between elements. Height is treated as constant across an element in this simulation, so the condition holds. Flow into unsaturated elements adjacent to the front boundary can be then be found by integrating the normal component of the linearly varying flux across the element edge. This allows for improved estimates of flow front progression without resorting to more computationally expensive mixed-methods.

The current simulation is restricted to planar geometries, but this is sufficient to capture the majority of key behaviour, and the extension to 2.5D shell geometries is relatively straightforward.

4 Structural problem

RTM Light mould compliance can potentially vary from near-rigid to very flexible due to differences in mould construction (e.g. material, thickness, use of stiffeners, etc.), part size, target volume fractions, and injection pressures. This paper considers the canonical RTM Light process, which has a rigid A-side mould, and a thin B-side mould constructed from a linearly elastic material. For planar geometries, the structural behaviour of this type of mould can be modelled by the Kirchhoff thin plate theory. This model requires that 1) the plate's thickness is small relative to its characteristic length, and 2) the deflections are small relative to the thickness. Both these conditions can be met by requiring the B-side mould to be constructed from a sufficiently stiff material.

In the case of isotropic, homogenous plates with a constant flexural rigidity D, deflection u is related to lateral distributed load b by

$$\nabla^4 u = \frac{b}{D} \qquad (3)$$

Analytical solutions to Eq. 3 exist for simple geometries and loading and boundary conditions. along with Green's functions for deflection for general loading states [8]. However, a useful RTM Light simulation requires deflection of non-regular mould geometries, as well as an ability to handle more advanced construction features, such as anisotropic materials, variable thickness, and the application of stiffeners. For these reasons, it is necessary to adopt a numerical solution procedure.

While a number of alternative numerical procedures are available for thin plate problems, such as the boundary element method, the finite element method is preferred in this simulation because of its numerical efficiency, established literature, and versatility. It is easily extended into 2.5D by adopting shell elements, and to thick plates by using those based on Reissner-Mindlin thick plate theory or 3D elasticity. Furthermore, many of the assembly and solver routines can be shared between the flow and structural finite element modules.

The plate bending element is the 9 DOF discrete Kirchhoff triangle (DKT), implemented using the local coordinate formulation given by Batoz [9]. While faster converging elements are available, the DKT is suitable for this simulation because of its reliability and low numerical overhead. Clamped, simple support, and free edge boundary conditions can be specified.

In the current simulation, the same mesh is used for the structural and flow problems. Deflections and loads are lumped in a consistent manner and passed between solvers during each iteration.

6 Coupling and solution procedure

The flow equation (Eq. 1) is coupled to the structural problem by the dependence of height and permeability on mould displacement u:

$$K = K(h, \mathbf{x}, t) \qquad (4)$$

$$h = u(\mathbf{x}, t) + h_0(\mathbf{x}) \qquad (5)$$

where h_0 is a reference height at zero deflection. Similarly, the structural problem is coupled to the flow problem by the dependence of the lateral load q on the resin pressure:

$$b = p_{ext} - (\sigma_f + p) \qquad (6)$$

where p_{ext} is the external loading (typically atmospheric pressure), σ_f is the fibre compaction stress and p is the resin pressure.

The iterative solution procedure used to solve the system is flowcharted in Fig. 3. The first stage is to determine the initial mould deflection for the dry preform, i.e. with a zero fluid pressure loading term:

$$b = p_{ext} - \sigma_f(u + h_0) \tag{7}$$

Once determined, the filling stage coupling algorithm begins by guessing $\dot{h}$, either by taking $\dot{h}$ from the previous time step or a linear interpolation of the previous two time steps. The guess value is passed to the flow module, and the fluid pressure, flux, and time step are calculated. The pressure is combined with the fibre compaction stress to determine the distributed load on the mould, which is then passed to the structural module. The calculated height profile and time step are used to update $\dot{h}$ using a backward difference discretisation. If the change in $\dot{h}$ is within tolerance, the flow front is updated and time is advanced; otherwise, the guess value of $\dot{h}$ is updated.

Initially the updated guess value was taken directly from the structural module result. However, this was found to produce large oscillations in the calculated pressure field. To reduce these oscillations, a weighting parameter ω was introduced, such that the updated guess was a weighted average of the calculated height and the previous guess:

$$\dot{h}_t^{i+1} = \omega \dot{h}_t^i + (1-\omega)\dot{h}_t^{i+1} \tag{8}$$

7 Numerical Studies

A series of numerical experiments have been conducted to test the efficacy of the simulation. Rates of convergence for the current coupling algorithm are slow, particularly for large mould deflections (>10% initial cavity height), and faster convergence is only available at the expense of stability. The cases presented here therefore only cover high rigidity moulds with small deflections. Despite this, the effects of mould compliance on LCM mould filling can still be observed.

Both cases are based on a 1 m x 1 m square mould, with a cavity height of 4.25 mm. The reinforcement parameters are based on an isotropic E-glass chopped strand mat (CSM). Compaction and permeability relations are based on experimental data presented by Walbran in [10]. For the permeability an exponential model is used:

$$K_{ii} = 3.07\times10^{-8}\exp(-12.97V_f)\ \text{m}^2 \tag{8}$$

and the compaction response is modelled with a fourth order polynomial:

$$\begin{aligned}\sigma_f &= 2.9\times10^5 - 3.7\times10^6 V_f \\ &\quad + 1.7\times10^7 V_f^2 - 3.6\times10^7 V_f^3 \\ &\quad + 3.0\times10^7 V_f^4\ \text{Pa}\end{aligned} \tag{9}$$

Other parameters are listed in Table 1. All studies used a constant pressure injection scheme, with no vacuum. This is equivalent to setting p_{ext} = 0. For each case four different upper mould thickness were considered: 35mm, 50mm, 75mm, and 100mm. The material properties for the upper mould were those of structural steel, with a Young's modulus of 200 GPa and a Poisson's ratio of 0.3. The mould thicknesses are at the upper end of the acceptable range for applying Kirchhoff plate theory, but this is not particularly crucial for these expository studies. A clamped boundary condition is applied to the mould edge.

7.1 Case 1: Rectilinear filling of a square mould

The first case considers rectilinear filling, with a line gate and vent along opposing sides. A 4096 element mesh right sided triangles was used. Only half the mould was meshed, with symmetry conditions for the plate and structural domain being applied to the centreline edge. Fig. 4 shows the mould cavity thickness for the 35 mm upper mould at the completion of filling. The peak deflection occurs at (0.5,0.45) – slightly behind the centre point of the mould – due to the fluid pressure gradient.

The symmetry line cavity thicknesses at the end of filling for all moulds are shown in Fig. 5. Peak deflections range from 8.23% to 0.4% of h_0. These thickness changes have little effect in the corresponding fluid pressures, as can be seen in Fig. 6. The small difference is likely due to the relatively small changes in permeability and porous volumes, even for the 35 mm mould.

Fill time as a function of normalised flexural rigidity is presented in Fig. 7. The fill time appears to converge towards the rigid (RTM) value as expected, but the convergence is from above, not from below

as would be expected with decreasing volume fraction and permeability. This may be a consequence of the true differences in fill time being within the approximation error of the flow front predictions. Further investigation into this behaviour is necessary.

7.2 Case 2: Radial filling of a square mould

The radial filling case – central injection with a perimeter gate – was analysed with a 2048 element quarter-square mesh of right sided triangles. Symmetry boundary conditions were applied on the left and bottom edges. Fig. 8 shows the mould deflections for the 35 mm mould at the end of filling across the entire mesh, and the end of filling deflection along a 45° line from the inlet is presented in Fig. 9 for each mould. The fluid pressure at the same points is given in Fig. 10 Compared with the rectilinear case, there is a larger difference in the fluid pressure profile as mould stiffness changes (Fig. 11). The direction of this change is consistent with experimentally observed data for axisymmetric RTM Light processes [11].

The behaviour of fill time with mould rigidity is more consistent with expectations for the radial filling case (Fig. 11), with fill times converging towards the rigid mould value from below. The sensitivity of fill time is much higher for the radial case, with fill times up to 14% faster than rigid mould case, compared to 2% difference for the same mould in rectilinear filling. This is likely due to the concentration of high fluid pressure near the center of the mould, resulting in larger bending moments and greater deflections. The greatest pressure drop occurs in this region, so the deflection and its effect on permeability have a maginified effect.

8 Conclusions and future work

A 2D simulation of the RTM Light composites manufacturing process has been described. It couples a finite element/control volume simulation fluid flow in deformable porous media with a plate-bending finite element solver, using elements based on the Kirchhoff thin plate theory. Results have been shown for two case studies – rectilinear and radial flow in a square mould. The simulation is showing qualitatively good results at low deflections, but numerical stability and convergence issues remain at larger deflections. Further development in this area is in progress, along with other improvements, such as the incorporation of the post-filling resin bleeding stage, extension to 2.5D shell structures, and experimental validation.

Table 1: Process parameters for case studies

Datum height, h_0	4.25 mm
Datum volume fraction, V_{f0}	0.410
Fluid viscosity	0.5 Pa.s
Injection pressure	5 bar
Vent pressure	1 bar

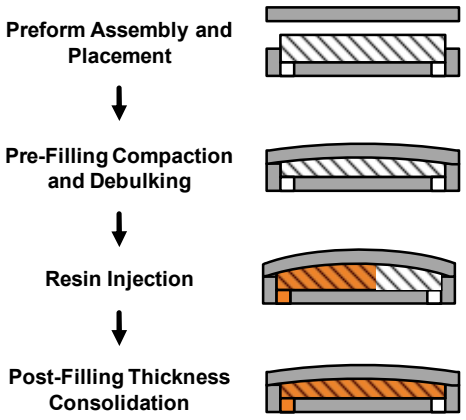

Fig. 1 Schematic of the RTM Light manufacturing process.

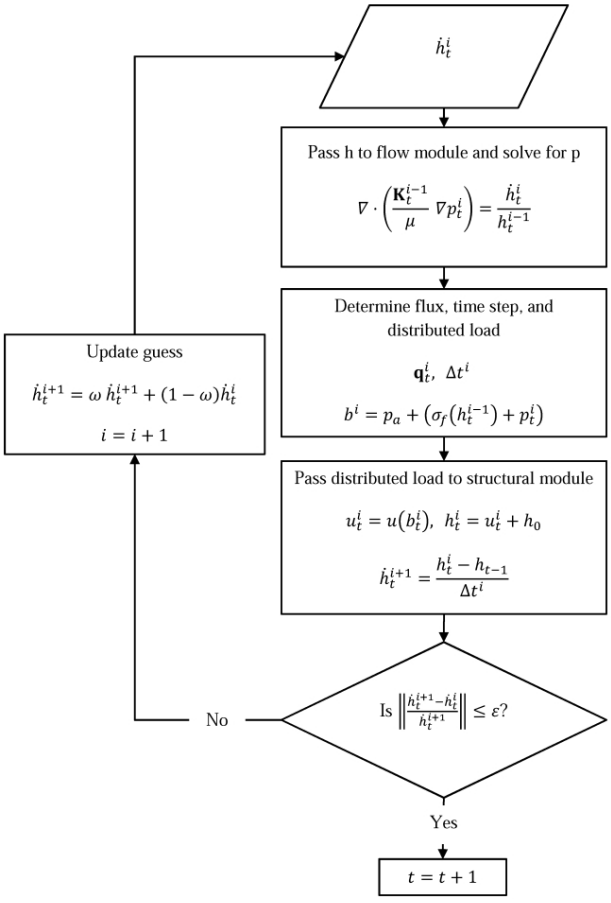

Fig. 2 Coupling algorithm flowchart

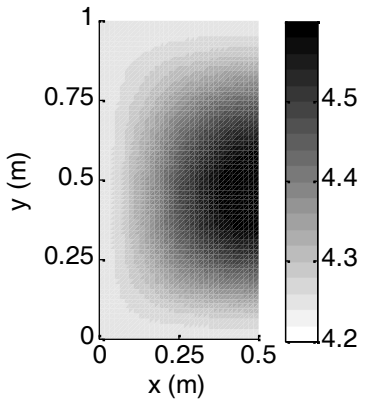

Fig. 3 Mould cavity thickness in mm at the end of filling. 35 mm upper mould. Rectilinear filling.

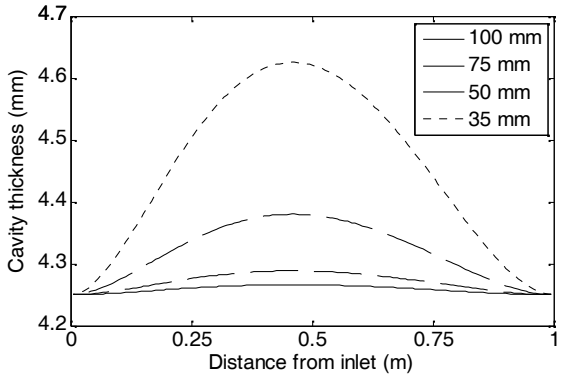

Fig. 4 Mould cavity thickness at the end of filling along the center line (x=0.5) for a range of upper moulds. Rectilinear filling.

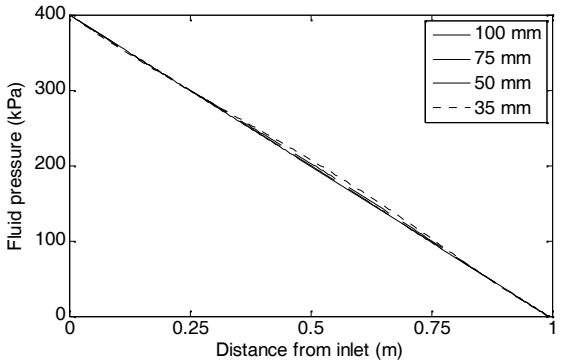

Fig. 5 Fluid pressure at the end of filling along the center line (x=0.5) for a range of upper moulds. Rectilinear filling

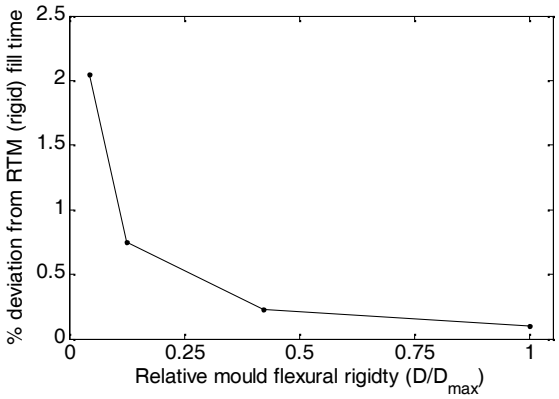

Fig. 6 Deviation in fill time as a function of mould flexural rigidity. Rectilinear filling.

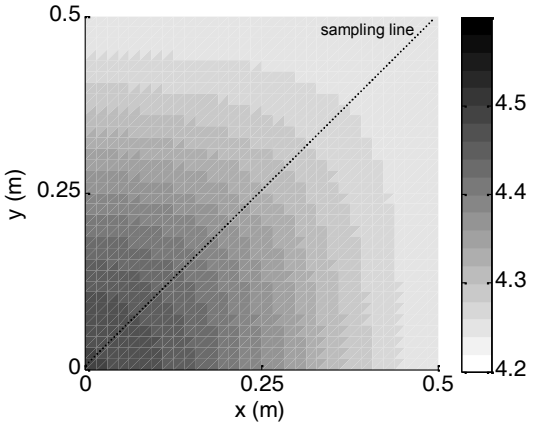

Fig. 7 Mould cavity thickness in mm at the end of filling. 35 mm upper mould. Radial filling.

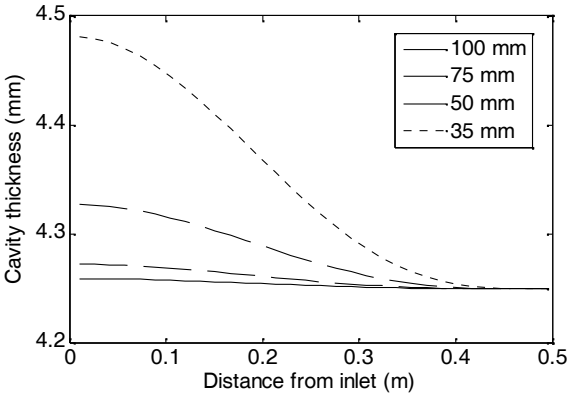

Fig. 8 Mould cavity thickness at the end of filling for a range of upper moulds. Radial filling.Samples are taken along the 45° line.

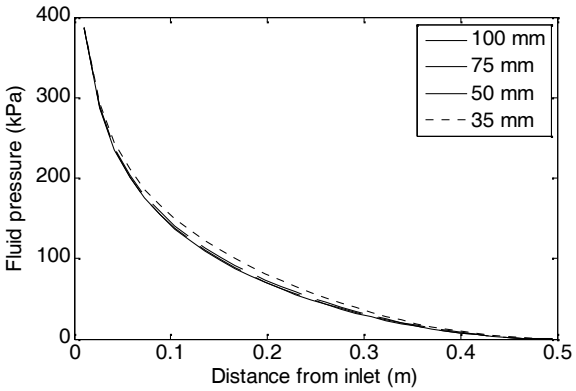

Fig. 9 Fluid pressure at the end of filling for a range of upper moulds. Radial filling.

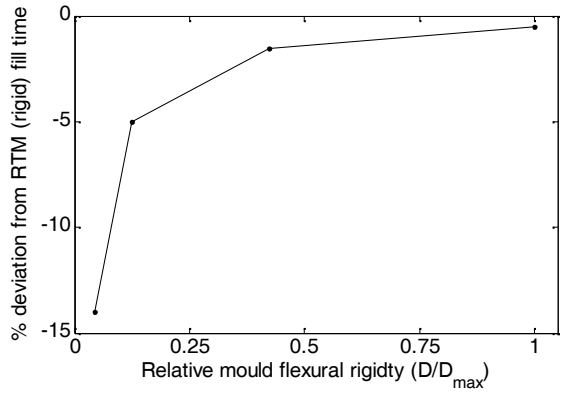

Fig. 10 Deviation in fill time as a function of mould flexural rigidity. Radial filling.

References

[1] M.V. Bruschke and S.G. Advani "A finite element/control volume approach to mold filling in anisotropic porous media". *Polymer Composites,* Vol. 11, No. 6, pp 398-405, 1990.

[2] F. Trochu, R. Gauvin and D.M. Gao "Numerical analysis of the resin transfer molding process by the finite element method". *Advances in Polymer Technology,* Vol. 12, No. 4, pp 329-42, 1993.

[3] Q. Govignon, S. Bickerton and P.A. Kelly "Simulation of the reinforcement compaction and resin flow during the complete resin infusion process". *Composites Part A: Applied Science and Manufacturing,* Vol. 41, No. 1, pp 45-57, 2010.

[4] P. Simacek and S.G. Advani "Desirable features in mold filling simulations for liquid composite molding processes". *Polymer Composites,* Vol. 25, No. 4, pp 355-67, 2004.

[5] F. Trochu, E. Ruiz, V. Achim and S. Soukane "Advanced numerical simulation of liquid composite molding for process analysis and optimization". *Composites Part A: Applied Science and Manufacturing,* Vol. 37, No. 6, pp 890-902, 2006.

[6] P.A. Kelly and S. Bickerton "A comprehensive filling and tooling force analysis for rigid mould LCM processes". *Composites Part A: Applied Science and Manufacturing,* Vol. 40, No. 11, pp 1685-97, 2009.

[7] P.A. Kelly and S. Jennings "Nonconforming Elements for Liquid Composite Molding Process Simulation". *Proceedings of 8th International Conference on Flow Processes in Composite Materials,* Douai, France, 2006.

[8] Y.A. Melnikov "Green's function of a thin circular plate with elastically supported edge". *Engineering Analysis with Boundary Elements,* Vol. 25, No. 8, pp 669-76, 2001.

[9] J.L. Batoz, K.J. Bathe and L.W. Ho "Study of three-node triangular plate-bending elements.". *International Journal for Numerical Methods in Engineering,* Vol. 15, No. 12, pp 1771-812, 1980.

[10] W.A. Walbran, B. Verleye, S. Bickerton and P.A. Kelly "Prediction and experimental verification of Normal Stress Distributions on Mould Tools During Liquid Composite Moulding". *Composites Part A: Applied Science and Manufacturing,* Vol. (In Press), No. pp 2011.

[11] J. Timms, Q. Govignon, S. Bickerton and P.A. Kelly "Observations from the filling and post-filling stages of axisymmetric liquid composite moulding with flexible tooling". *Proceedings of FPCM 10,* Ascona, 2010.